Hindawi
International Journal of Aerospace Engineering
Volume 2022, Article ID 2109994, 15 pages
https://doi.org/10.1155/2022/2109994

Research Article

A More Precise Modeling Method for Pneumatic Cabin Pressure Control System considering the Ambient Environmental Impacts

Yonggui Zheng, Meng Liu, Junjun Zhuang, and Hao Wu

School of Aeronautic Science and Engineering, Beihang University, Beijing 100191, China

Correspondence should be addressed to Hao Wu; haowu@buaa.edu.cn

Received 14 May 2022; Revised 8 July 2022; Accepted 14 July 2022; Published 30 July 2022

Academic Editor: Jinchao Chen

Pneumatic cabin pressure control system (PCPCS), with its exceptional electromagnetic compatibility, is expected to become the major equipment on a high-performance airplane again in the future. Although the PCPCS has been mature for a long time, the broad popularization of the digital cabin pressure control system (DCPCS) has left the PCPCS in the cold for decades. This makes the PCPCS unable to meet the severe cabin pressure regulation requirements of high-speed aircraft today. For this purpose, a more precise PCPCS modeling method is proposed. Through this method, the relation between different parts in the PCPCS can be accurately characterized. Moreover, the impact of the ambient environment on the PCPCS is taken into consideration. This method can be used to accurately analyze the PCPCS under maneuvering flight. And it also assists in the verification of the system improvements of dynamic performance in the future. Simulation results show that the aircraft acceleration disturbs the PCPCS slightly, and the cabin air inflow fluctuation has a significant impact on the cabin air pressure.

1. Introduction

Before the first practical pressurized cabin airplane Lockheed XC-35 [1] came into being, the open cockpit had been used on the airplane for about 30 years, and the pilot's operating environment could not be protected at that time. Since the 1930s, pressurized aircraft have developed rapidly, and the cabin pressure control system (CPCS) came out.

The Garrett Corporation has made outstanding contributions to the development of the pneumatic cabin pressure control system (PCPCS). The "Kemper" style cabin pressure control invested by James Kemper [2] was widely used in PCPCS at that time. And the balanced poppet outflow valve advanced by Raymond Jenson [3] and Richard Fischer [4] was the most recognized cabin outflow valve and is still in use at present. These two masterpieces built the prototype of PCPCS. Operation of the PCPCS is completely pneumatic, depending on the cabin pressure and the ambient pressure.

Soon after the emergence of the PCPCS, electric motors and digital controllers spread rapidly with the popularization of electrification [5]. Digital cabin pressure control system (DCPCS), with its programmability and simple structure, grows quickly. Extensive research has been conducted on the control strategy [6], the controller structure [7, 8], the system flow [9], and the system analysis and improvements [10, 11]. These work promoted the application of the DCPCS. Programmable digital controllers and electric butterfly valves can be found on nearly every modern aircraft especially on commercial aircraft.

Although the DCPCS has become mainstream, the PCPCS, with its exceptional electromagnetic compatibility and fast response, plays an irreplaceable role in some high-speed aircraft. Until now, the pneumatic outflow valves are still used in many airplanes as safety valves [12].

In 2009, a Lockheed Martin F-22 raptor was reported to have been killed by a Boeing EA-18G Growler in a simulated combat exercise (https://www.key.aero/forum/modern-military-aviation/90802-growler-power-ea-18g-boasts-f-22-kill-photos). This big news made researchers realize the importance of electromagnetic warfare. And avionics is possible to be exposed to the danger of electromagnetic interference at any time. The PCPCS, with its inherent superb

electromagnetic compatibility, has a great opportunity to become the focus of future research again.

The CPCS is of vital importance because it is closely related to crew comfort [13], even aircraft safety [14, 15]. Even though the CPCS has been developed for decades, barotrauma caused by cabin pressure fluctuations/spikes has always plagued pilots [16–18]. It is reported that the Boeing F/A-18E/F Super Hornet suffered cabin pressure fluctuations (https://news.usni.org/2019/04/04/navy-rules-out-contamination-as-physiological-episodes-cause-focused-on-air-pressure-as-super-hornet-rates-still-high). And the spikes in cockpit's cabin pressure were also reported on the Lockheed Martin F-35 Lightning II (https://www.defensenews.com/smr/hidden-troubles-f35/2020/04/24/the-pentagon-has-cut-the-number-of-serious-f-35-technical-flaws-in-half). One of the main reasons for the spikes in the cabin is the deficiencies of the CPCS. The deficiencies make the air pressure and rate of pressure change in the cabin fail to meet the related criteria [19]. Obviously, engineers need to put forward specific improvements to eliminate the fluctuations. The engineering experience and a large number of tests could be the only way to solve the problem. This leads to the urgency of a more reliable and higher performance CPCS.

It is important to thoroughly investigate the internal mechanism of the CPCS. As the DCPCS is widespread, the amount of related research is considerable. But this is not the case with PCPCS. The PCPCS matured in the 1960s-1970s. But the dynamic performance of modern aircraft has developed by leaps and bounds. While the analysis of the PCPCS is still based on the linear, steady-state, and approximate model, and the transient cabin outflow rate is always difficult to match the inflow rate during maneuvering flights, more in-depth research is needed to update the dynamic performance of PCPCS, so as to adapt to modern advanced aircraft.

Most related PCPCS research mainly focuses on the enhancement of the prototype. Burgess et al. [20] put forward a new pressure control system combined with a pneumatic amplifier relay. Whitney et al. [21] presented an improved PCPCS that is adapted to prevent the difference between cabin pressure and atmospheric pressure from exceeding a threshold value. Horner et al. [12] introduced a poppet outflow valve with an integrated metering valve poppet as the controller. These new systems/valves have made some changes to meet additional requirements such as quick response, anti-icing, and dust filtration. The working principle of these optimized pneumatic cabin pressure control systems remains unchanged. It could be summarized as follows: cabin-to-ambient pressure differential acts on the diaphragm to open/close the valve, and the compressed spring is used to balance the force on the diaphragm; pressure differential can be regulated by the pressure controller working as a throttle valve.

Modeling and simulation were also carried out to describe the system. Zheng [22] studied a cabin pneumatic pressure control system and analyzed the dynamic characteristics systematically. Chaurasiya et al. [23] developed a dynamic model of a cabin pressure control system and studied the steady-state and transient flight conditions using MATLAB. These works help describe the pneumatic cabin pressure control system and analyze the system characteristics. But the models are linearized and idealized. Wei [24] studied the flow characteristics inside the outflow valve using the user-defined function (UDF) of the Fluent software. But the work did not build the relationship between the outflow valve and the cabin pressure. The pressure fluctuation in the cabin is a fast and transient phenomenon. Classical linearized and approximate methods are more suitable for steady-state analysis and are difficult to demonstrate the phenomenon.

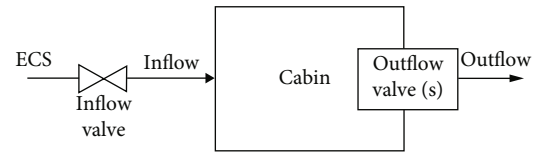

Figure 1: Diagram view of cabin pressure.

It is apparent that pressure fluctuations/spikes appear during maneuvering flight. In order to understand the internal mechanism of the pneumatic pressure control system and find the causes of fluctuations, two aspects are significant: (1) build a more precise system model. An accurate model helps analyze the internal relation between different components in the system. (2) Take into account the impact of the external environment on PCPCS. Under transient flight conditions, the ambient environment could interfere with the PCPCS.

In this paper, a more accurate model is carried out, especially the balanced poppet outflow valve. Pressure distribution on the valve, which affects the movement of the main poppet, is discussed. External environmental impacts are also studied, including the acceleration of the airplane and the cabin transient inflow.

This paper is organized as follows. Section 2 discusses the basic system flow of PCPCS. In Section 3, ambient environmental impacts on the system are discussed. A precise model of the PCPCS is put forward in Section 4. Simulation examples are provided in Section 5 to demonstrate pressure spikes. Section 6 draws the conclusion of the paper.

2. System Flow of the PCPCS

The PCPCS has been developing for decades. The structure and components evolved gradually and finally matured in the 1960s [4, 25]. Figure 1 shows how the PCPCS controls the cabin pressure. The air pressure of an aircraft cabin is mainly affected by cabin inflow and outflow. Airflow treated by the environmental control system (ECS) is controlled by the inflow valve and then enters the cabin. Outflow valves are used to exhaust airflow from the cabin. In most cases, PCPCS works to modulate airflow from the cabin to atmosphere by regulating the opening of the outflow valves. Normally, redundant outflow valves are installed to improve reliability. In terms of system working principles, there is no essential distinction between one outflow valve and multiple valves. So, in this paper, modeling and analysis are carried out based on one outflow valve.

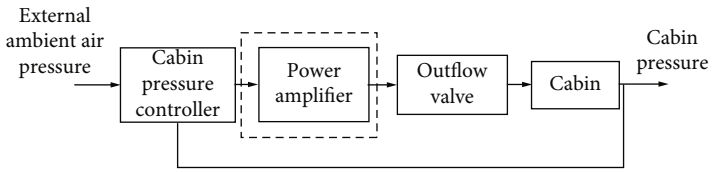

Figure 2: Schematic diagram of pneumatic cabin pressure control system.

The block diagram of the PCPCS is shown in Figure 2. The cabin pressure controller compares the air pressure between the cabin and the ambient environment. Then, the pneumatic signal from the controller is transmitted to the outflow valve. A pneumatic relay, which is an optional component, works as a power amplifier to amplify the gas mass flow between the controller and the outflow valve. The outflow valve receives the signal and then raises and lowers, thereby modulating the airflow from the cabin to the ambient environment. This system flow is basic but important. Almost every PCPCS of aircraft is based on this system flow now. Last but not the least, the PCPCS is fully automated, and no additional automation equipment is required. The control law is reflected in the hardware parameters of the system.

The outflow valve is the actuator of the system; its schematic diagram is shown in Figure 3. Pneumatic signal (air stream) flows into the control chamber to change the air pressure in the control chamber. Then, the differential pressure inside and outside the actuator diaphragm drives the poppet to move upward and downward. Thus, the exhaust airflow from the cabin is regulated, and the cabin pressure is limited. When the atmospheric pressure is greater than cabin pressure, it will push the balance diaphragm to move upward. Then, the outflow valve opens, and atmospheric air flows into the cabin to reduce the cabin-to-atmosphere differential pressure. There are some valves with guiding shafts [3, 12] to ensure poppet stability. And some valves integrate the controller in the outflow valve [4]. Even so, the working principle is the same. So, the outflow valve analysis in this paper is based on the model illustrated in Figure 3.

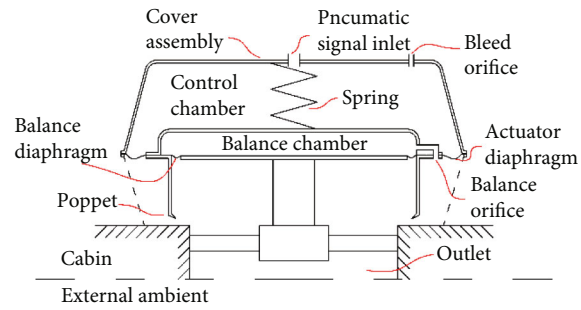

Figure 3: Schematic diagram of the outflow valve.

3. Environmental Impacts on the PCPCS

Unlike the digital cabin pressure control system, the PCPCS is purely mechanical and pneumatic. Consequently, interactions among the components could be disturbed by the environment.

(1) Acceleration affects the deformation of elastic elements. Gravity was ignored in most research because the moving parts in the PCPCS are usually installed horizontally. But when it comes to maneuvering flight, the acceleration in flight direction is often several times the gravitational acceleration. As a result, there will be an additional "inertial force" applied to the moving part when the airplane accelerates or decelerates

(2) The flow field near the outlet of the outflow valve is complicated. The pressure distribution near the C-shape cross-section poppet determines the force on the diaphragms. But most of the early literary works used a nozzle model to compute the mass flow rate of the outflow valve and regarded the pressure near the outlet of the outflow valve as a constant. This leads to deviations in calculation results. Carrying out flow tests is helpful, but the process is complex and time-consuming

(3) The amount of engine bleeding air fluctuates during maneuvering flight, sometimes causing cabin air inflow fluctuation. The inflow fluctuation leads to cabin air pressure fluctuation and then results in cabin pressure control system oscillation. Although the inflow fluctuation does not exactly belong to an ambient environment factor for an aircraft, it does disturb the PCPCS

Figure 4 shows the environmental impacts on the PCPCS during the maneuvering flight. Acceleration changes, valve outlet pressure distribution, and inflow fluctuations affect the cabin pressure jointly. In the following part of this paper, studies are carried out to analyze these impacts.

4. Numerical Model and Method

4.1. Model of the PCPCS. A classic cabin pressure controller consists of two sections: the isobaric pressure section and the differential pressure section (as shown in Figure 5). The poppet of the isobaric pressure section is initially open, and the vacuum bellow is elastic. When the flight altitude increases, ambient environmental pressure decreases. Then, the bellow expands, and the effective flow area of the poppet valve in the isobaric pressure section is reduced. As the flight altitude continues to increase, the differential pressure section begins

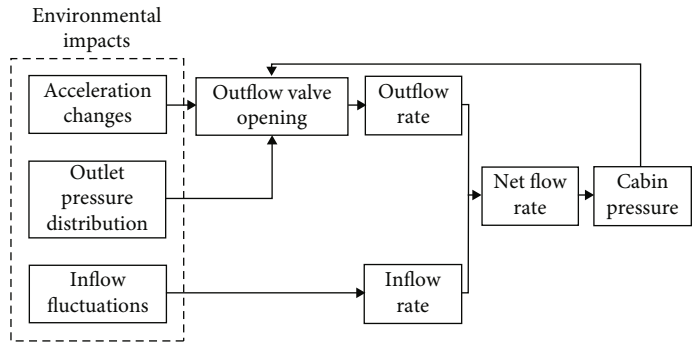

Figure 4: Environmental impacts on the PCPCS.

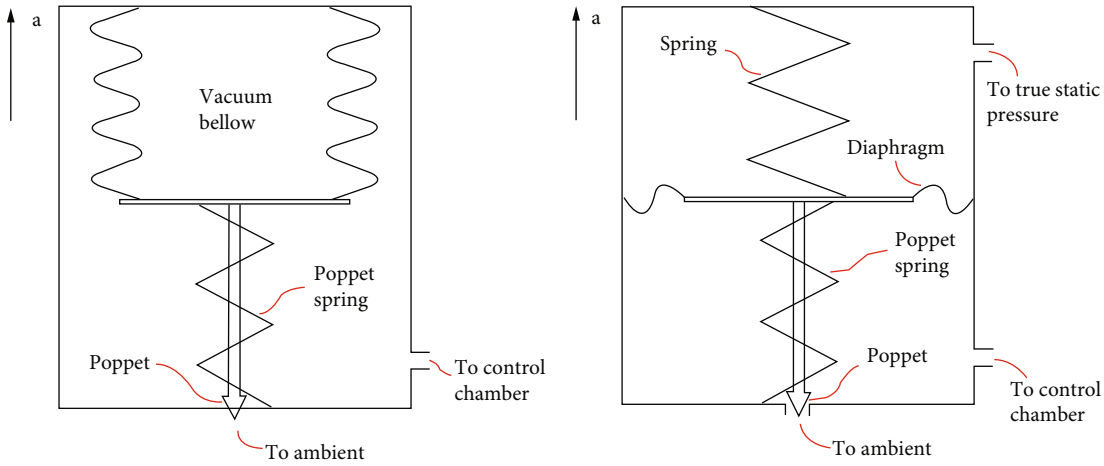

(a) Isobaric pressure section

(b) Differential pressure section

Figure 5: Schematic diagram of the cabin pressure controller.

to work. Differential pressure on both sides of the diaphragm pushes the poppet to open. The poppets of both sections work as a throttle and control the pressure in the control chamber of the outflow valve. Here, we say that the cabin pressure controller transmits the pneumatic signal to the outflow valve.

For convenience, assume that the acceleration of the aircraft is "a" shown in Figure 5. An additional inertial force is applied to each component. The equation of motion for the poppet in the isobaric pressure section can be described as follows:

$$m_i\ddot{y}_i = F_{\mathrm{is}} - F_{ib} - F_{ir} - F_{ipd} - F_{iI}. \tag{1}$$

As the elastic elements are connected to the poppet, the deformation of these elastic elements is consistent with the opening of the poppet. So, the forces in Equation (1) can be given by:

$$\begin{cases} F_{\mathrm{is}} = K_{is}\bullet(y_{i\,\max} - y_i) + F_{\mathrm{is}0} - m_{\mathrm{is}}\ddot{y}_{\mathrm{is}} - f_{\mathrm{is}}\dot{y}_{\mathrm{is}} - m_{\mathrm{is}}\mathrm{a}, \\ F_{ib} = m_{ib}\ddot{y}_{ib} + \mathrm{f}_{ib}\dot{y}_{ib} + K_{ib}\bullet(y_{i\,\max} - y_i) + F_{ib0} + m_{ib}\mathrm{a} + f_{ib}\dot{y}_{ib} - \mathrm{P}_{cc}\bullet A_b, \\ F_{ir} = f_i\dot{y}_i, \\ F_{ipd} = \Delta\mathrm{P}_{ip}A_{ip}, \\ F_{iI} = m_i a. \end{cases} \tag{2}$$

It should be noted that the y_{ib} is the displacement of the mass center of the elastic vacuum bellow. So, the relation between y_{ib} and y_i is

$$dy_{ib} = \frac{dy_i}{2}. \tag{3}$$

The equation of motion for the poppet in the differential pressure section can be described as follows:

$$m_d\ddot{y}_d = F_{dps} - F_{ds} + F_{dd} - F_{dpd} + F_{dr} - F_{dI}. \tag{4}$$

Similarly, the forces in Equation (4) can be represented by:

$$\begin{cases} F_{dps} = K_{dps}\bullet(y_{d\,\max} - y_d) + F_{dps0} - m_{dps}a - m_{dps}\ddot{y}_{dps} - f_{dps}\dot{y}_{dps}, \\ F_{ds} = K_{ds}\bullet(y_{d\,\max} - y_d) + F_{ds0} + m_{ds}\ddot{y}_{ds} + m_{ds}a + f_{ds}\dot{y}_{ds}, \\ F_{dd} = (P_{cc} - P_{ts})\bullet A_d, \\ F_{dpd} = \Delta\mathrm{P}_{dp}\bullet A_{dp}, \\ F_{dr} = f_d\bullet\dot{y}_d, \\ F_{dI} = m_d a. \end{cases} \tag{5}$$

The opening of the poppets in the isobaric pressure section and differential pressure section is obtained using the equations above. And the mass flow rate of the cabin pressure controller can be calculated by classical isentropic nozzle flow equations.

After computing the "pneumatic signal" from the controller, we should compute the output of the actuator—the opening of the outflow valve. Likewise, assume that the outflow valve shown in Figure 3 is placed in a noninertial reference frame, and the acceleration is also upward with magnitude "a." The motion of the outflow valve poppet is given by the following equations:

$$\begin{aligned} & m_v \ddot{y}_v = F_{vad} + F_{vbc} - F_{vs} - F_{vbd} - F_{vr} - F_{vI}, \\ & \begin{cases} F_{vad} = (P_{ad} - P_{cc}) A_{ad}, \\ F_{vbc} = (P_{bc} - P_{cc}) A_{bc}, \\ F_{vs} = m_{vs} \ddot{y}_{vs} + K_{vs} \bullet (y_{v\,\max} - y_v) + F_{vs0} + m_{vs} a + f_{vs} \dot{y}_{vs}, \\ F_{vbd} = (P_{bc} - P_{bd}) A_{bd}, \\ F_{vr} = f_v \bullet \dot{y}_v, \\ F_{vI} = m_v a. \end{cases} \end{aligned} \tag{6}$$

Based on the equations above, we know how the outflow valve poppet moves when the control chamber pressure P_{cc} changes. However, it should be noted that the volume of the control chamber varies as the poppet moves upward and downward. And so does the balance chamber. Therefore, volume changes should be taken into consideration when computing the air pressure in the chambers.

The air pressure in the control chamber is expressed using the ideal gas equation state:

$$\frac{d(P_{cc} V_{cc} / R T_{cc})}{dt} = \frac{dm_{cc}}{dt}. \tag{7}$$

The right side of Equation (7) is the mass change of the air in the control chamber. It can be obtained by the 1-dimensional (1D) isentropic nozzle flow equations [26]. The temperature change is so small that it can be ignored. Thus, the left side of Equation (7) can be expanded to:

$$\frac{d(P_{cc} V_{cc} / R T_{cc})}{dt} = \frac{V_{cc}}{R T_{cc}} \frac{dP_{cc}}{dt} + \frac{P_{cc}}{R T_{cc}} \frac{dV_{cc}}{dt}. \tag{8}$$

If we want to calculate the pressure change in the control chamber, we have to know how the volume of the control chamber changes. Assume that the poppet is initially closed, that is, $y_v = 0$. When the poppet moves upward, it comes to $y_v + dy_v$, and the reduction of the control chamber volume is $dV_{cc} = A_{cc} dy_v$. The bottom of the control chamber can be approximated by a circular surface. The base area of the control chamber varies with y_v, as illustrated in Figure 6.

We describe it with a linear approximation:

$$A_{cc} = A_{cc\,\max} - y_v \frac{A_{cc\,\max} - A_{cc\,\min}}{y_{v\,\max}}, \tag{9}$$

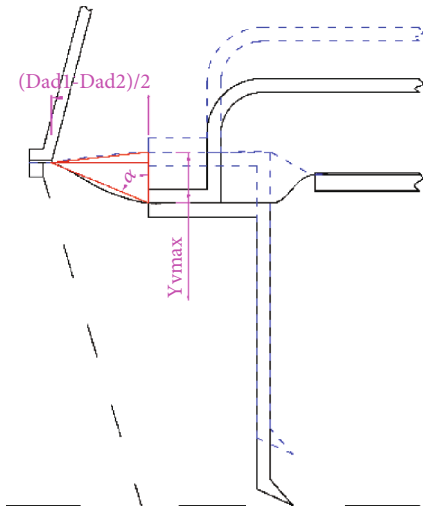

Figure 6: Schematic diagram of the moving poppet.

Table 1: Permutation of valve opening, ambient pressure, and differential pressure.

	Simulation conditions				
Relative valve opening, x	0.1	0.25	0.5	0.75	1
Ambient pressure, P_a (kPa)	101	80	60	40	20
Differential pressure, P_d (kPa)	3	10	15	20	30

where the minimum base area is:

$$A_{cc\,\min} = \frac{\pi}{4} D_{ad1}^2. \tag{10}$$

And the maximum base area can be estimated by the trigonometric function:

$$A_{cc\,\max} = \frac{\pi}{4} D_{ad2}^2 + \frac{\pi}{4} \frac{D_{ad1}^2 - D_{ad2}^2}{\sin \alpha}. \tag{11}$$

We can calculate $\sin \alpha$ with equations below:

$$\tan \alpha = \frac{(D_{ad1} - D_{ad2})/2}{y_{v\,\max}}, \tag{12}$$

$$\sin \alpha = \frac{\tan \alpha}{\sqrt{1 + \tan^2 \alpha}}. \tag{13}$$

With Equations (9)–(13), we can obtain the relation between A_{cc} and y_v. For simplicity, we use the equation below:

$$A_{cc} = \text{Const} + K_{cc} \bullet y_v, \tag{14}$$

where "*Const*" in the equation represents a constant and "K_{cc}" is a scale factor less than 0. Then, we can describe the relation between V_{cc} and y_v through the equation:

$$dV_{cc} = (\text{Const} + K_{cc} \bullet y_v) dy_v. \tag{15}$$

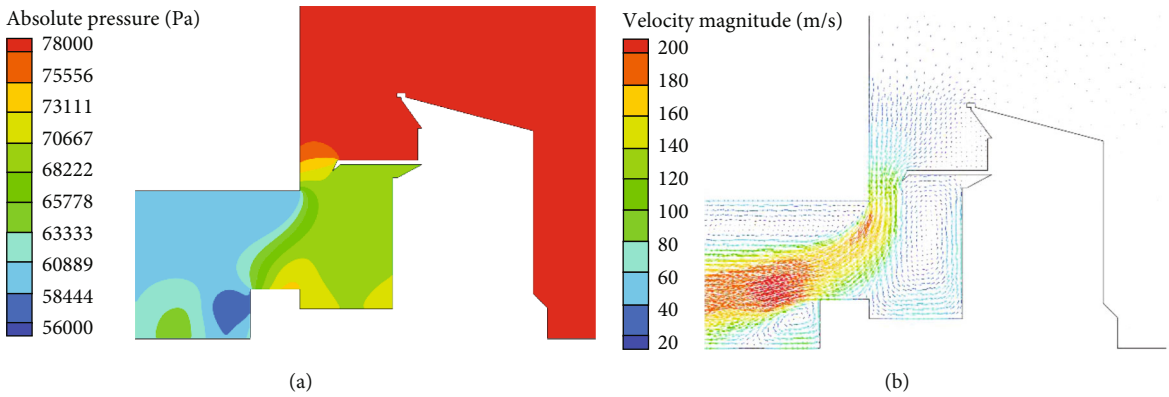

Figure 7: CFD study on the flow field near the outlet of the outflow valve (opening = 10 mm, ambient pressure = 60 kPa, differential pressure = 20 kPa), (a) pressure distribution, (b) velocity vectors.

Consequently, the air pressure in the control chamber can be obtained. And the air pressure in the balance chamber is obtained in the same way.

As for the air pressure in the cabin, it can be described with

$$\frac{V_c}{RT_c}\dot{P}_c = M_{\text{in}} - M_{\text{out}}. \tag{16}$$

At this point, the opening of the outflow valve can be calculated. In order to calculate the mass flow rate of air leaving the cabin, the relation between the valve opening and mass flow rate is vital. Most of the early literary works used the isentropic nozzle model to estimate the mass flow rate of the outflow valve. But actually, the airflow through the C-shaped cross-section poppet is complex. Moreover, the flow field near the outflow valve affects pressure distribution, which in turn affects the force of the diaphragms. But traditional models regarded the pressure on the lower surface of the balance diaphragm P_{bd} as ambient environment pressure. So, a more precise analysis of the force and airflow for the PCPCS is necessary.

4.2. Pressure Distribution near the Outflow Valve. Since the outflow valve is the core actuator of the cabin pressure control system, additional attention needs to be paid to the interaction of the outflow valve and the airflow. Computational fluid dynamics (CFD) studies were carried out to analyze the pressure distribution near the outlet of the outflow valve. Three variables are considered to find the law of pressure distribution: opening of the valve, ambient air pressure, and differential pressure in the cabin. For a general outflow valve, the travel is about 20 mm. What is more, generally speaking, the flight altitude is not higher than 10 km when the differential pressure section starts to work. The pressure at that altitude is not greater than 20 kPa. Thirdly, the maximum cabin-to-ambient differential pressure is about 30 kPa. Under these circumstances, 150 simulation tests were carried out based on the permutation of the three variables, as shown in Table 1.

As the computational load is massive for a 3D simulation, a 2D rotational axis-symmetric mesh was put into use. Figure 7 is the pressure distribution near the outflow valve when the valve opening is 10 mm, the ambient pressure is 60 kPa, and the differential pressure is 20 kPa. It can be seen that the pressure distribution near the actuator diaphragm seems to be close to the pressure in the cabin. But the pressure near the balance diaphragm is different from the outlet pressure because the airflow is treated by the poppet.

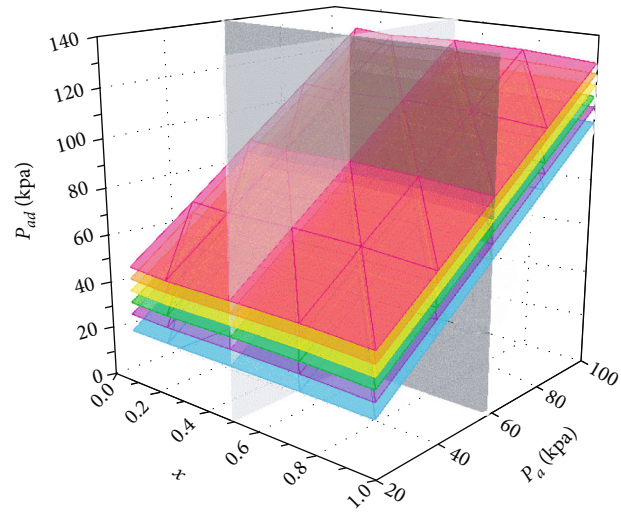

Figure 8: Relation of actuator diaphragm pressure P_{ad} with relative valve opening x and ambient pressure P_a.

We summarized the simulation results of 150 working conditions and collected the data including average air pressure near the actuator diaphragm P_{ad}, average air pressure data near the balance diaphragm P_{bd}, and the mass flow rate data of the valve M_{out}. The collected data are illustrated in Figures 8–16.

Figure 8 provides the interrelations among P_{ad}, x, P_a, and P_d. Figure 9 is the 2D plot results from Figure 8 intersection with the plane $x = 0.5$. Figure 10 is the 2D slice of Figure 8 at $P_a = 60$ kPa. It is apparent from Figures 8 and 9 that the P_{ad} is close to but slightly less than P_c. And as shown in Figure 10, x has little effect on P_{ad}. But with the increase of x, the P_c line waves slightly. A possible explanation for

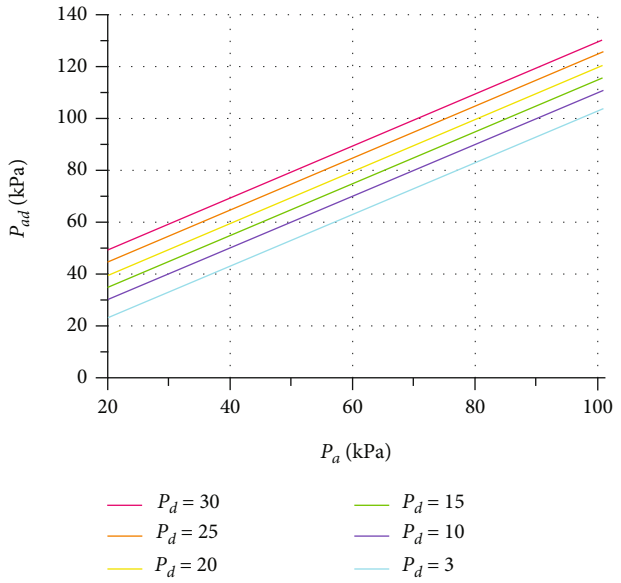

Figure 9: Relation between actuator diaphragm pressure P_{ad} and ambient pressure P_a at different differential pressure P_d.

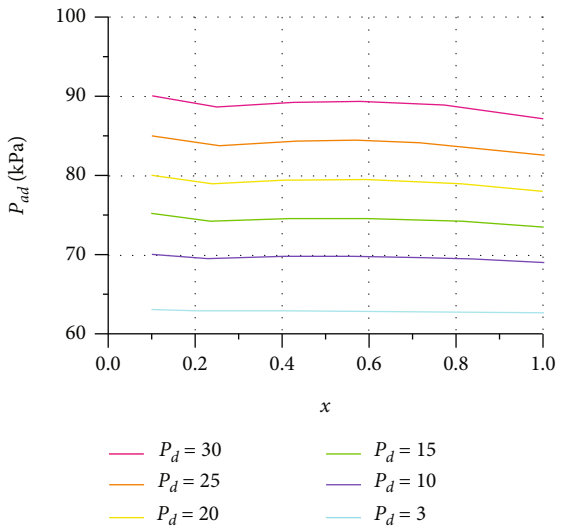

Figure 10: Relation between actuator diaphragm pressure P_{ad} and relative valve opening x at different differential pressure P_d.

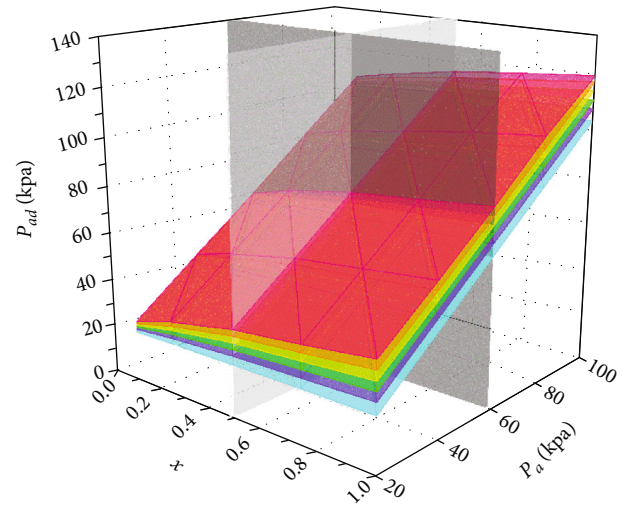

Figure 11: Relation of balance diaphragm pressure P_{bd} with relative valve opening x and ambient pressure P_a.

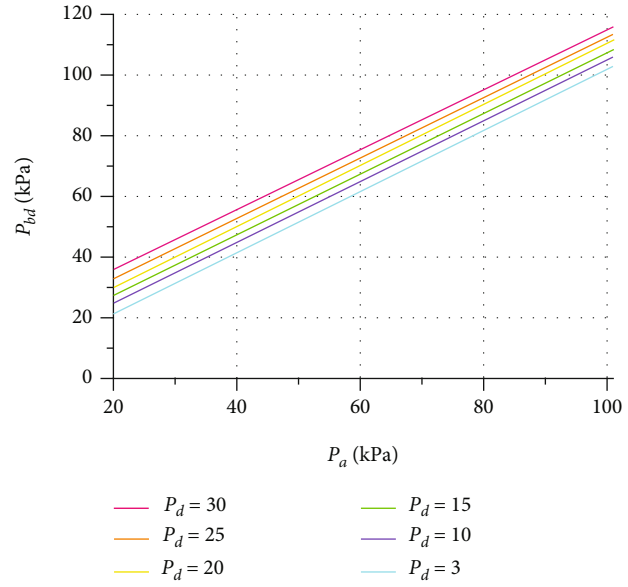

Figure 12: Relation between balance diaphragm pressure P_{bd} and ambient pressure P_a at different differential pressure P_d.

this might be that the flow field near the actuator diaphragm is relatively stable and is less influenced by the poppet movement and differential pressure of the outflow valve.

Figure 11 shows the correlations among P_{bd}, x, P_a, and P_d. Figure 12 is the 2D line when cutting Figure 11 with plane $x = 0.5$. And Figure 13 is the slice of Figure 11 cut by the plane $P_a = 60$ kPa. As can be seen from the figures, P_{bd} is higher than P_a. What is more, the larger the value of x, the greater the pressure difference between P_{bd} and P_a. It can also be seen from the figures that P_{ad} increases as P_d increases. These relationships may partly be explained by the airflow influence on the balance diaphragm. As the poppet moves upward, the influence area of the high-pressure airflow in the cabin increases, which increases the air pressure of the balance diaphragm.

Figure 14 shows the change in mass flow rate M_{out}. The curve in Figure 15 is the surface in Figure 14 cut by plane $x = 0.5$. The curve illustrated in Figure 16 is obtained by the intersection of the plane $P_a = 60$ kPa and the surface in Figure 14. In theory, the outflow valve is linear. This is consistent with what is shown in Figure 15. However, as the opening of the valve increases, the increasing trend of mass flow slows down. A possible explanation for this might be that the increasing opening of the valve causes more intense vortices, which bring energy loss and reduce the flow capacity of the valve.

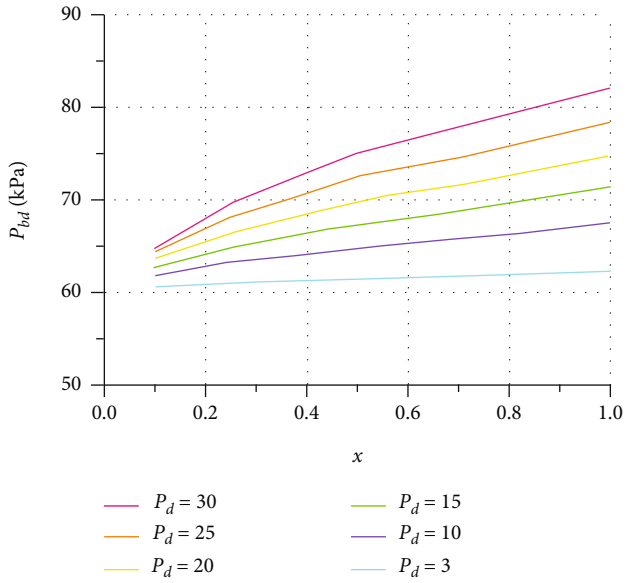

Figure 13: Relation between balance diaphragm pressure P_{bd} and relative valve opening x at different differential pressure P_d.

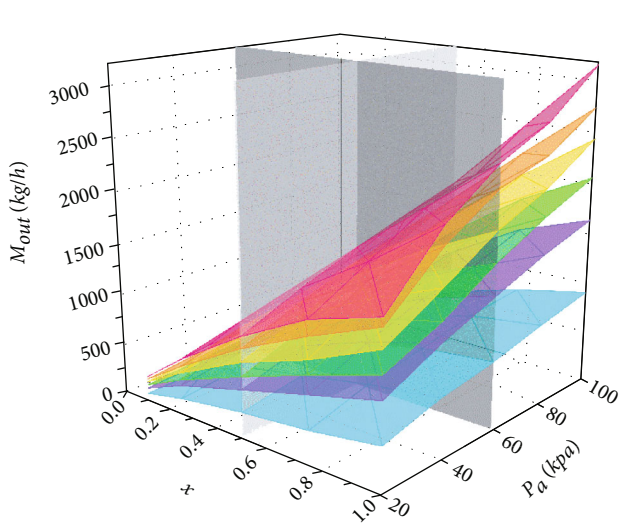

Figure 14: Relation of mass flow rate M_{out} with relative valve opening x and ambient pressure P_a.

The results of the CFD studies indicate that:

(i) The pressure under the actuator diaphragm is hardly affected by the movement of the poppet. Because the actuator diaphragm is far away from the outlet of the outflow valve

(ii) The pressure under the balance diaphragm is affected by the complex flow near the outlet of the outflow valve. This in turn changes the resultant force on the poppet

(iii) The complex flow near the valve outlet also disturbs the air outflow and distorts the flow characteristics of the outflow valve

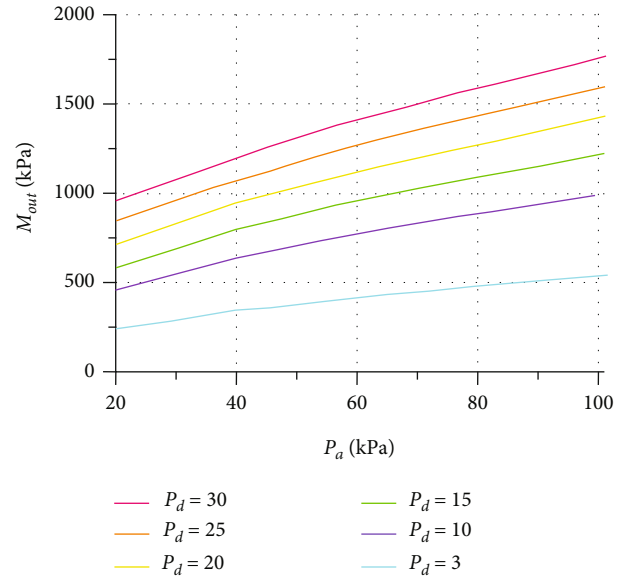

Figure 15: Relation between mass flow rate M_{out} and ambient pressure P_a at different differential pressure P_d.

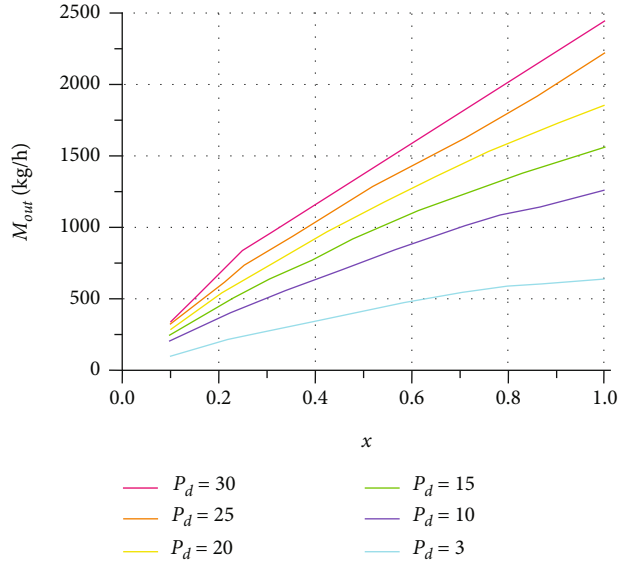

Figure 16: Relation between mass flow rate M_{out} and relative valve opening x at different differential pressure P_d.

These working conditions may not be the actual conditions, but the above simulations help to summarize the law of the outflow valve to regulate the airflow. The nonlinear fitting tool is used to fit the above data, so as to obtain P_{ad}, P_{bd}, and M_{out} under different working conditions. Then, the dynamic models described above are able to characterize the movement of the pneumatic cabin pressure control system.

4.3. Calculating Method for PCPCS under Maneuvering Flight. Up to now, a system-level research method has been established. A mathematical model of the PCPCS is built considering the ambient environmental impacts. CFD

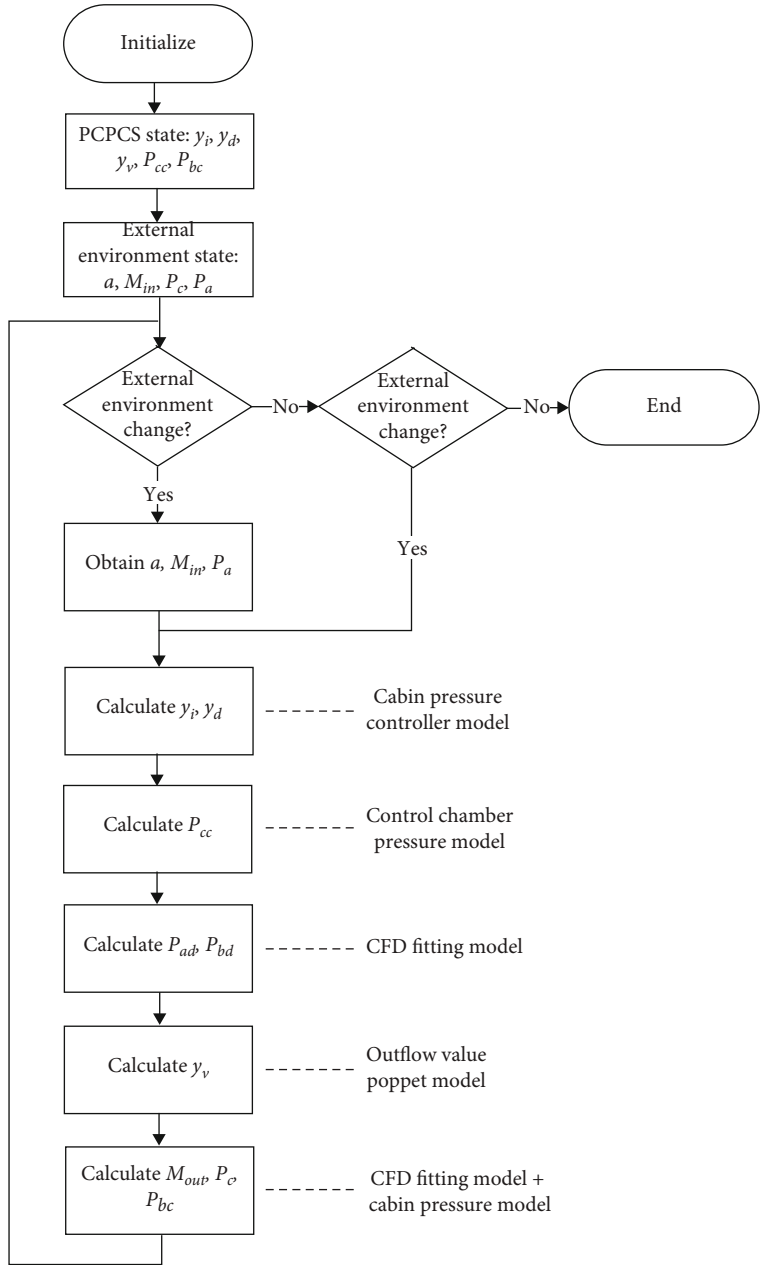

Figure 17: Computing process for PCPCS under maneuvering flight.

simulations were carried out to calculate the accurate pressure near the diaphragms and the mass flow rate of the outflow valve. Thus, the working process of the PCPCS under maneuvering flight is obtainable.

Figure 17 is the computing process for the PCPCS when the aircraft is maneuvering. At the beginning of calculation, the initial state of the PCPCS and the essential environmental parameters should be confirmed. When the aircraft starts maneuvering, the external environment changes. Under a given aircraft acceleration "a," the airspeed around the plane is obtainable. Then, the static pressure near the outlet of the outflow valve "P_{ts}," which is the ambient environment pressure, can be calculated according to the altitude. And the mass flow entering the cabin M_{in} is known according to the aircraft ECS. Due to the aircraft's acceleration, the resultant force of the poppets in the cabin pressure controller would change. Then, the opening of the poppets, which are "y_i" and "y_d," can be calculated using the model above (Although the isobaric pressure section and differential pressure section usually do not work simultaneously, here, we mention them together for the sake of convenience). Accordingly, the pressure signal, which is the airflow rate between the controller and control chamber, can be calculated, and the pressure in the control chamber "P_{cc}" is obtained. Using the fitting results of the CFD simulations, the pressure under the actuator diaphragm P_{ad} and the balance diaphragm P_{bd} can be obtained. And consequently, the opening of the outflow valve "y_v" can be calculated using the

dynamic equation of the poppet. So, the outflow rate "M_{out}" of the valve is easy to know based on the fitting results of the CFD simulations, and the cabin pressure is obtained. Then, the pressure in the balance chamber can be calculated through nozzle flow equations. And these state parameters of the PCPCS are determined at this iteration step. The iteration stops until the PCPCS state and the external environment no longer change.

5. Simulation and Discussion

The method presented in this paper helps to analyze the PCPCS under maneuvering flight. In order to demonstrate how the ambient environment acts on the PCPCS, an imaginary flight mission is provided to show the performance of the PCPCS. Before the imaginary flight mission simulation, real measured flight data from a training flight is used to prove the effectiveness of our modeling method.

5.1. Model Verification. Cui [27] provided the real case of an aircraft full afterburner takeoff. The cabin inflow rate and the cabin pressure are shown in Figures 18 and 19. The red dash lines represent the data measured during the flight. And the black solid lines are the data simulated based on the model presented in this paper.

The cabin inflow rate increases from 100 kg/h to 900 kg/h during about 4 s, leading to the boost of the cabin pressure. The delay of the sensor causes a phase difference between the simulation and the measurement. And the sampling interval of the pressure sensor is 1 s, which makes the red curve not as smooth as the black curve. Figure 19 indicates that the simulation results reflect the change law of the cabin pressure accurately. What is more, due to the limitation of the sampling frequency of the pressure sensor, the red curve does not show the peak value of the pressure change rate, while the black curve shows it clearly. It also points out that the real pressure change in the cabin could be more severe than the measurements.

5.2. Flight Mission Simulation. After the model verification, we provide an extreme imaginary flight mission to show how the PCPCS works transiently. The initial flight altitude is 1 km, and the speed is 250 m/s. The plane starts to accelerate at time $t = 1\,s$. At time $t = 11\,s$, the plane flies at a constant speed of 387 m/s. The plane begins to decelerate at time $t = 15\,s$. The flight speed recovers to 250 m/s at time $t = 27\,s$. The speed and the acceleration are shown in Figure 20. Simulated airflow fluctuation entering the cabin is illustrated in Figure 21 to represent the potential instability of the ECS. The relative opening of the outflow valve and the cabin pressure are shown in Figure 22.

Initially, the cabin pressure is maintained at about 90 kPa. When the plane starts to accelerate, the cabin inflow increases, and the cabin pressure increases dramatically. Then, the pressure difference on both sides of the outflow valve actuator diaphragm rises, pushing the outflow valve to open. At time $t = 2.5\,s$, the cabin inflow rate decreases, but the cabin pressure is still too high, so the outflow valve keeps opening. When the cabin pressure drops to less than

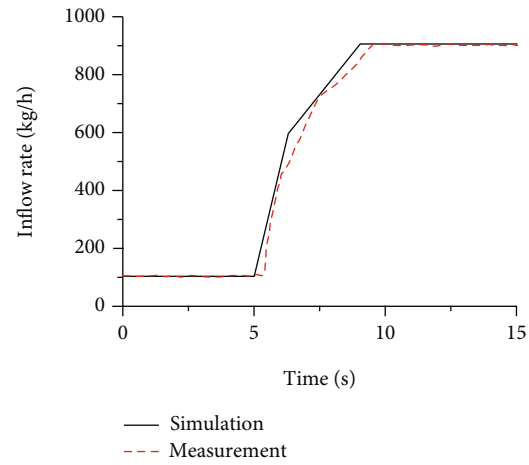

Figure 18: Comparison between the simulated and measured data of cabin inflow rate.

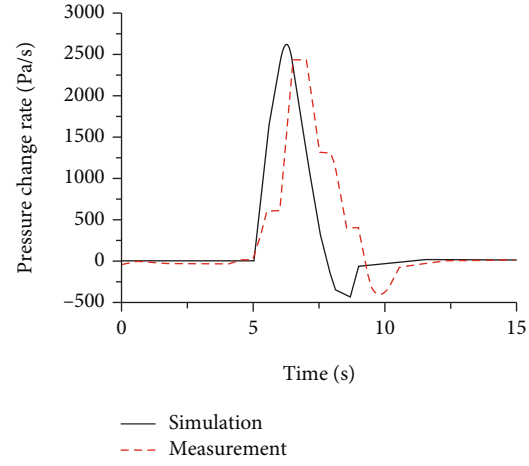

Figure 19: Comparison between the simulated and measured data of cabin pressure change rate.

90 kPa, the valve starts to close. And gradually, the valve reaches the equilibrium point—about 45% relative opening. At time $t = 15\,s$, the cabin inflow fluctuates again, and the outflow valve adjusts automatically to regulate the cabin pressure to 90 kPa. During the whole mission, air pressure in the control chamber P_{cc} maintains at 90 kPa. The inertial force has little effect on the poppets of the cabin pressure controller because the elasticity coefficients of the springs are large.

As mentioned above, aircraft acceleration could disturb the force on the PCPCS. But the cabin pressure fluctuation shown in Figure 22 is the synthetic result of aircraft acceleration and cabin air inflow. So, we separate the effects of these two factors to observe how they disturb the PCPCS, respectively. Figure 23 is the relative opening of the outflow valve influenced by the aircraft acceleration and the cabin inflow rate separately. The red line shows the relative opening of the outflow valve influenced by aircraft acceleration. And the blued line is the relative opening of the outflow valve influenced by cabin inflow. The dash line is the relative opening of the outflow valve influenced by these two factors

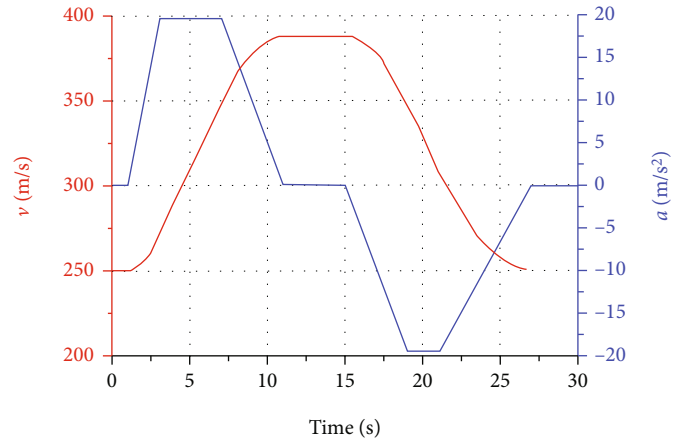

Figure 20: Aircraft speed and acceleration.

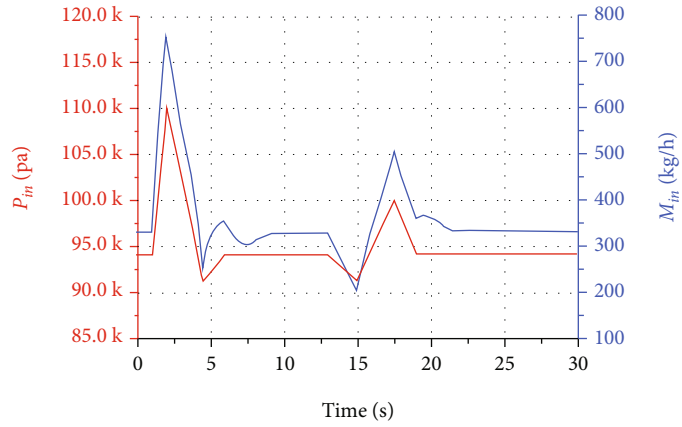

Figure 21: Cabin inflow fluctuation: inlet pressure and mass flow.

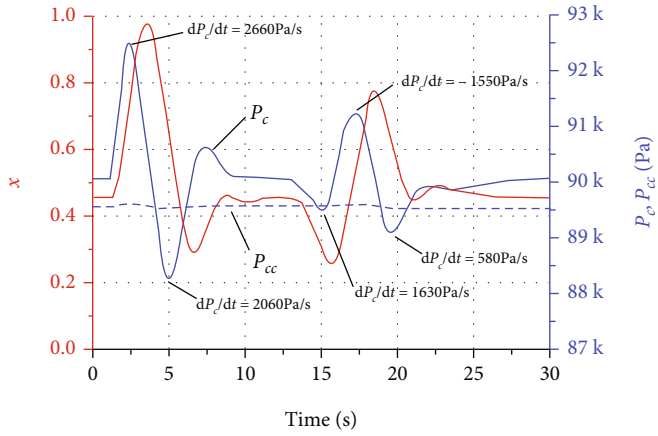

Figure 22: Relative opening of the outflow valve and the cabin pressure.

synthetically. So, it is with the cabin pressure lines in Figure 24, except for an additional dash line representing the pressure in the control chamber.

When the aircraft accelerates, the inertia force acts as a factor driving the outflow valve to close and driving the cabin pressure to rise. But the surge in cabin inflow, which significantly increases the cabin air pressure, pushes the outflow valve to open remarkably. So, the increase of the valve opening (the dash line in Figure 23) at time $t = 3\,s$ is the superposition effect of the two factors. At time $t = 18\,s$, the aircraft decelerates, and the inertia force pushes the outflow valve to open. So, we can find that the dash line is higher than the blue line at time $t = 18\,s$ because of the superposition effect. The pressure shown in Figure 24 reflects the

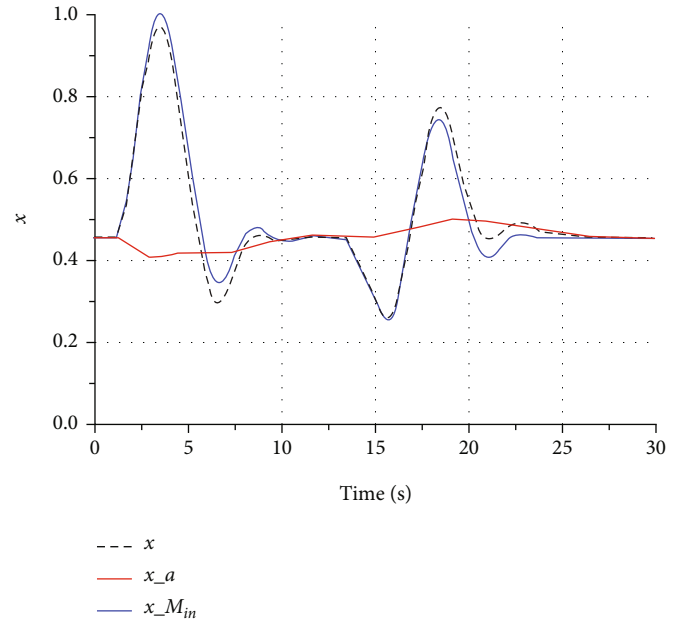

Figure 23: Relative opening of the outflow valve influenced by different ambient environmental factors.

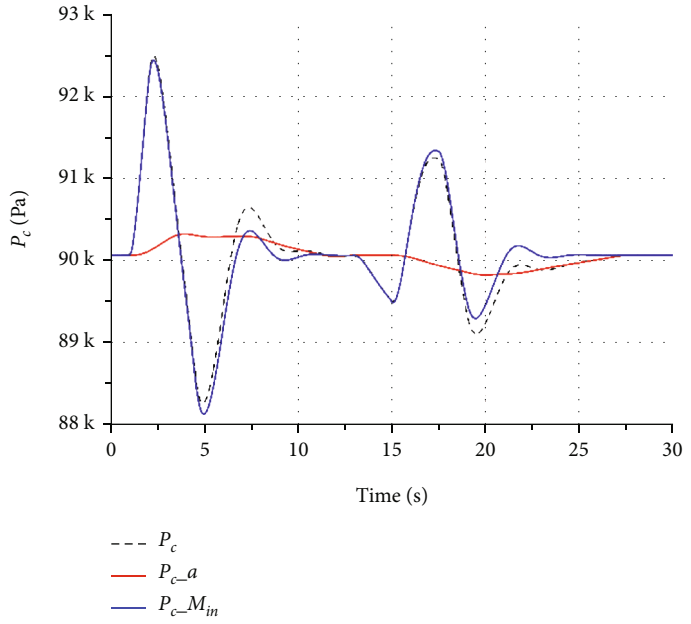

Figure 24: Cabin pressure influenced by different ambient environmental factors.

superposition effect of the cabin inflow and cabin outflow and is also the synthetic result of the cabin inflow rate and the outflow valve opening. Comparing these two figures, it can be found that the change in cabin pressure is always earlier than the change in the opening of the outflow valve. This result can be explained in part by the passive regulating structure of the PCPCS.

From the simulation results above, we find that aircraft acceleration would disturb the PCPCS. But the impact of the cabin inflow rate fluctuation is more drastic. The pressure change rates shown in Figure 22 indicate that the PCPCS model used in this section does not meet the requirements of the relative cabin pressurization criteria. A possible explanation for these results is the limitations of the dynamic capabilities of the PCPCS. Another possible explanation for this is that the cabin volume does not match the cabin inflow rate.

In a word, the modeling method presented in this paper can not only reveal the relation of each part of the PCPCS but also reflect the influence of the ambient environment on the PCPCS during maneuvering flight. This helps analyze the PCPCS and improve its performance to meet the strict requirements of modern aircraft.

Finally, it should be clear that the modeling discussed in this paper cannot represent all current pneumatic pressure

control systems on aircraft. But their working principles and physical structures are similar. The method provided in this paper gives a new approach to analyzing the pneumatic pressure control system.

6. Discussion

The model presented in this paper shows great accuracy and demonstrates the dynamic process of the PCPCS under maneuvering flights. There are other modeling methods to describe the PCPCS. The dynamic modeling methods of the PCPCS are similar, but there are several key points between our methods and others:

(i) The acceleration of the aircraft does affect the action of the outflow valve. The main reason why an outflow valve is installed horizontally is to eliminate the influence of its gravity on the actions. But the components of the PCPCS could be affected by the acceleration of the aircraft during maneuvering flights. Previous modeling methods did not consider this factor

(ii) As mentioned before, the 1D isentropic nozzle model is not suitable for the calculation of the mass flow rate of the outflow valve with a specially shaped poppet. The CFD simulations help calculate the mass flow rate as accurately as possible. And it helps to establish a fitting model to calculate the mass flow under different conditions

(iii) The outflow valve is a complex mechanism, the pressure distribution on the diaphragms is different under different working conditions. The previous study approximated the pressure on the diaphragms to the cabin pressure or the ambient pressure; this leads to inaccurate conclusions about the PCPCS. The CFD simulations in this paper help to find the pressure distribution law of the outflow valve and describe the PCPCS more precisely

7. Conclusion

In this paper, a new modeling method for pneumatic cabin pressure control system was proposed. This method took the influence of ambient environment change on the PCPCS during maneuvering flight into consideration. The interference of aircraft acceleration on PCPCS was discussed. And it was pointed out that the flow field near the outlet of the outflow valve affects the pressure distribution of the diaphragms. The inertia force was added to the dynamic modeling of each part in the PCPCS. And CFD studies were carried out to solve the accurate pressure distribution near the outlet of the outflow valve. Numerical simulations showed that the instantaneous acceleration of the aircraft disturbs the PCPCS, and the fluctuation of the cabin inflow rate has the most noticeable impact on cabin pressure. The method presented in this paper is good at analyzing the internal relations of each part of the PCPCS and is helpful for PCPCS improvement to meet the requirements of modern aircraft.

Nomenclature

ΔP_{dp}: Pressure difference between inlet and outlet of the poppet, in the differential pressure section
ΔP_{ip}: Pressure difference between inlet and outlet of the poppet, in the isobaric pressure section
a: Airplane acceleration
A_{ad}: Effective area of the actuator diaphragm
A_b: Bottom area of the vacuum bellow, in the isobaric pressure section
A_{bc}: Area of the surface connecting the control chamber and the balance chamber
A_{bd}: Effective area of the balance diaphragm
A_{cc}: Bottom area of the control chamber
$A_{cc\ \max}$: Maximum bottom area of the control chamber
$A_{cc\ \min}$: Minimum bottom area of the control chamber
A_d: Diaphragm area, in the differential pressure section
A_{dp}: Effective area of the poppet, in the differential pressure section
A_{ip}: Effective area of the poppet, in the isobaric pressure section
D_{ad1}: External diameter of the actuator diaphragm
D_{ad2}: Internal diameter of the actuator diaphragm
F_{dd}: Force generated by the pressure difference on both sides of the diaphragm, in the differential pressure section
F_{dI}: Inertia force on the poppet, in the differential pressure section
F_{dpd}: Force generated by the static pressure difference acting on the poppet, in the differential pressure section
F_{dps}: Force of the poppet spring on the poppet, in the differential pressure section
F_{dps0}: Initial force of the poppet spring on the poppet, in the differential pressure section
F_{dr}: Resistive force acting on the poppet, in the differential pressure section
F_{ds}: Force of the spring on the poppet, in the differential pressure section
F_{ds0}: Initial force of the spring on the poppet, in the differential pressure section
F_{ib}: Force of the vacuum bellow on the poppet, in the isobaric pressure section
F_{ib0}: Initial force of the vacuum bellow on the poppet, in the isobaric pressure section
F_{iI}: Inertia force on the poppet, in the isobaric pressure section
F_{ipd}: Force generated by the static pressure difference acting on the poppet, in the isobaric pressure section
F_{ir}: Resistive force acting on the poppet, in the isobaric pressure section
F_{is}: Force of the spring on the poppet, in the isobaric pressure section
$F_{\mathrm{is}0}$: Initial force of the spring on the poppet, in the isobaric pressure section
F_{vad}: Force generated by the pressure difference on both sides of the actuator diaphragm, in the outflow valve

F_{vbc}: Force generated by the pressure difference between the control chamber and the balance chamber, in the outflow valve
F_{vbd}: Force generated by the pressure difference on both sides of balanced diaphragm, in the outflow valve
F_{vI}: Inertia force on the poppet, in the outflow valve
F_{vr}: Resistive force acting on the poppet, in the outflow valve
F_{vs}: Force of the spring on the poppet, in the outflow valve
F_{vs0}: Initial force of the spring on the poppet, in the outflow valve
f_{dps}: Viscous resistance coefficient of the poppet spring, in the differential pressure section
f_{ds}: Viscous resistance coefficient of the spring, in the differential pressure section
f_i: Viscous resistance coefficient of the poppet, in the isobaric pressure section
f_{ib}: Viscous resistance coefficient of the vacuum bellow
f_{is}: Viscous resistance coefficient of the poppet spring, in the isobaric pressure section
f_v: Viscous resistance coefficient of the poppet, in the outflow valve
f_{vs}: Viscous resistance coefficient of the spring, in the outflow valve
K_{dps}: Elasticity coefficient of the poppet spring, in the differential pressure section
K_{ds}: Elasticity coefficient of the spring, in the differential pressure section
K_{ib}: Elasticity coefficient of the vacuum bellow, in the isobaric pressure section
K_{is}: Elasticity coefficient of the spring, in the isobaric pressure section
K_{vs}: Elasticity coefficient of the spring, in the outflow valve
M_{in}: Mass flow of the air entering the cabin
M_{out}: Mass flow of the air leaving the cabin through the outflow valve
m_{cc}: Mass of the air in the control chamber
m_d: Mass of the poppet, in the differential pressure section
m_{dps}: Mass of the poppet spring, in the differential pressure section
m_{ds}: Mass of the spring, in the differential pressure section
m_i: Mass of the poppet, in the isobaric pressure section
m_{ib}: Mass of the vacuum bellow, in the isobaric pressure section
m_{is}: Mass of the poppet spring, in the isobaric pressure section
m_v: Mass of the poppet, in the outflow valve
m_{vs}: Mass of the spring, in the outflow valve
P_{ad}: Pressure on the lower surface of the actuator diaphragm
P_{bd}: Pressure on the lower surface of the balance diaphragm
P_{bc}: Air pressure in the balance chamber
P_c: Air pressure in the cabin
P_{cc}: Air pressure in the control chamber
P_{in}: Pressure at the inlet of the inflow valve
P_{ts}: True static pressure at the current altitude
R: Specific gas constant for air
T_c: Air temperature in the cabin
T_{cc}: Air temperature in the control chamber
V_c: Volume of the cabin
V_{cc}: Volume of the control chamber
v: Aircraft speed
x: Relative opening of the outflow valve
y_d: Opening of the poppet, in the differential pressure section
$y_{d\ \max}$: Travel of the poppet, in the differential pressure section
y_{dps}: Displacement of the poppet spring center of mass, in the differential pressure section
y_{ds}: Displacement of the spring center of mass, in the differential pressure section
y_i: Opening of the poppet, in the isobaric pressure section
y_{ib}: Displacement of the poppet spring center of mass, in the isobaric pressure section
$y_{i\ \max}$: Travel of the poppet, in the isobaric pressure section
y_{is}: Displacement of the poppet spring center of mass, in the isobaric pressure section
y_v: Opening of the poppet, in the outflow valve
$y_{v\ \max}$: Travel of the poppet, in the outflow valve
y_{vs}: Displacement of the spring center of mass, in the outflow valve.

Data Availability

No data were used to support this study.

Conflicts of Interest

The authors declare that they have no conflicts of interest.

References

[1] A. Marchiando, "The Lockheed XC-35 and Harry Armstrong, MD: development of the first practical pressurized cabin airplane," *Aerospace Medicine and Human Performance*, vol. 88, no. 7, pp. 703-704, 2017.

[2] P. J. Taylor, "Cabin pressure control systems for general aviation aircraft," *SAE Transactions*, vol. 89, pp. 2124–2135, 2017.

[3] R. W. Jensen and The Garrett Corporation, "Safety valve," 1954, US Patent 2,672,086.

[4] R. A. Fischer and The Garrett Corporation, "Pressure regulating mechanism," 1961, US Patent 2,986,990.

[5] H.-U. Ettl, "Modern digital pressure control system," in *Digital Avionics Systems Conference*, p. 3948, San Jose, CA, USA, 1988.

[6] T. R. Arthurs, D. W. Horner, A. R. Laing, J. P. Rabon, and Honeywell International Inc, "Cabin pressure control system and method that accommodates aircraft take-off with and without a cabin pressurization source," 2008, US Patent 7.462,098.

[7] B. Petri, C. Felsch, V. Albrecht, L. Runkel, and Nord Micro AG and Co oHG, "Controller, cabin pressure control system and method of controlling cabin pressure," 2004, US Patent 6,676,504.

[8] F. R. Emmons, T. W. Donahue, and Raytheon Technologies Corp, "Adaptive aircraft cabin pressure control system," 1993, US Patent 5,273,486.

[9] D. Horner, B. Olson, G. McCoy, and Honeywell International Inc, "Multiple outflow valve cabin pressure control system," 2014, US Patent 8,864,559.

[10] D. Horner, T. Biss, G. McCoy et al., "Cabin pressure control system with multiple outflow valves and method of calibrating the outflow valve position feedback during flight," 2014, US Patent 8,694,181.

[11] W. Yan and D. Zhang, "Modeling and performance analysis of digital electronic-pneumatic cabin pressure control system," *Journal of Nanjing University of Aeronautics & Astronautics*, vol. 3, pp. 324–328, 2008.

[12] T. R. Darrell Horner, B. A. Arthurs, and Honeywell international Inc, "Poppet valve for cabin pressure control systems," 2013, US Patent 8,382,035.

[13] J. M. Muhm, P. B. Rock, D. L. McMullin et al., "Effect of aircraft-cabin altitude on passenger discomfort," *New England Journal of Medicine*, vol. 357, no. 1, pp. 18–27, 2007.

[14] T. Robinson, J. S. Evangelista, E. Latham, S. T. Mukherjee, and A. Pilmanis, "Recurrence of neurological deficits in an F/A-18D pilot following loss of cabin pressure at altitude," *Aerospace Medicine and Human Performance*, vol. 87, no. 8, pp. 740–744, 2016.

[15] K. J. Lee and A. Z. Sanou, "Decompression sickness in the F/A-18C after atypical cabin pressure fluctuations," *Aerospace Medicine and Human Performance*, vol. 89, no. 5, pp. 478–482, 2018.

[16] Y. Dou, X. Xu, H. Feng et al., "The effects of rapid altitude decompression on the middle ear and hearing," *Journal of Audiology and Speech Pathology*, vol. 19, no. 3, pp. 210–212, 2011.

[17] X. Xu, X. Ma, Y. Zhang, and Z. Jin, "Analysis of data of nasal cavity and nasal sinus of physical examination for change to equipment in pilots," *Journal of Audiology and Speech Pathology*, no. 3, pp. 210–212, 2008.

[18] Z. Jin, X. Xu, S. Zhang, and Y. Liu, "Clinical research on alternobaric vertigo in the flying environment," *Journal of Audiology and Speech Pathology, No.*, vol. 3, pp. 210–212, 2008.

[19] SAE, *Aircraft Cabin Pressurization Criteria*, SAE International, 2015.

[20] G. A. Burgess, P. J. Taylor, and Garrett Corp, "Pressure control system," 1976, US Patent 3,974,752.

[21] T. J. Whitney, T. L. Lui, and Honeywell International Inc, "Aircraft cabin multi-differential pressure control system," 2006, US Patent 7,066,808.

[22] X. Zheng, *Key Technology and Optimization of Pneumatic Cabin Pressure Regulating System, [Ph.D. thesis]*, Polytechnical University, Xi'an, China, 2016.

[23] K. L. Chaurasiya, B. Bhattacharya, A. K. Varma, and S. Rastogi, "Dynamic modeling of a cabin pressure control system," *Proceedings of the Institution of Mechanical Engineers, Part G: Journal of Aerospace Engineering*, vol. 234, no. 2, pp. 401–415, 2020.

[24] X. Wei, *Simulation of Pressure Regulation System of Aircraft Cabin, College of Aerospace Engineering, [M.S. thesis]*, Nanjing University of Aeronautics and Astronautics, Nanjing, China, 2012.

[25] L. F. Mauldin, R. C. Nelson, and Garrett Corp, "Pressure regulating mechanism," 1961, US Patent 2,986,989.

[26] M. J. Moran and H. N. Shapiro, *Fundamentals of Engineering Thermodynamics*, Wiley, Hoboken, NJ, USA, 2006.

[27] C. Cui, "Analysis and research on the growth rate of cabin pressure," *China Science & Technology Panorama Magazine*, no. 20, pp. 183-184, 2013.